Chinese Journal of Natural Medicines

Highly oxidized sesquiterpenoids from *Parasenecio rubescens* and assessment of their cytotoxicity

An JIN, Fangfang DUAN, Hanli RUAN

Citation: An JIN, Fangfang DUAN, Hanli RUAN, Highly oxidized sesquiterpenoids from *Parasenecio rubescens* and assessment of their cytotoxicity, Chinese Journal of Natural Medicines, 2024, 22(11), 1–10. doi: 10.1016/S1875-5364(24)60607-2.

View online: https://doi.org/10.1016/S1875-5364(24)60607-2

Available online at www.sciencedirect.com

ScienceDirect

Chinese Journal of Natural Medicines 2024, **22**(11): 1020-1029
doi: 10.1016/S1875-5364(24)60607-2

Chinese Journal of Natural Medicines

•Original article•

Highly oxidized sesquiterpenoids from *Parasenecio rubescens* and assessment of their cytotoxicity

JIN An[1, 2Δ], DUAN Fangfang[1Δ], RUAN Hanli[1*]

[1] *Hubei Key Laboratory of Natural Medicinal Chemistry and Resource Evaluation, School of Pharmacy, Tongji Medical College, Huazhong University of Science and Technology, Wuhan 430030, China;*
[2] *School of Pharmaceutical Sciences, Hunan University of Medicine, Huaihua 418000, China*

Available online 30 Nov., 2024

[ABSTRACT] A phytochemical investigation of the whole plant of *Parasenecio rubescens* (S. Moore) Y. L. Chen yielded 14 previously undescribed, highly oxidized bisabolane-type sesquiterpenoids, named pararunines L–Y, along with one known oplopane-type sesquiterpenoid. The structural elucidation of these compounds was accomplished through comprehensive spectroscopic analysis, including nuclear magnetic resonance (NMR) and high-resolution electrospray ionization mass spectrometry (HR-ESI-MS) techniques. Motivated by traditional uses and previous studies on this genus, all isolated compounds were subjected to *in vitro* cytotoxicity assays against four human cancer cell lines (MCF-7, Hela, HCT116, and HT-29). Considering that the reported chemical constituents of numerous other species within this genus primarily consist of eremophilane-type sesquiterpenoids, our findings not only expand the structural diversity of bisabolane-type sesquiterpenoids but also contribute valuable scientific evidence to the chemotaxonomy of this genus.

[KEY WORDS] *Parasenecio rubescens*; Asteraceae; Bisabolane-type sesquiterpenoids; Oplopane-type sesquiterpenoid; Cytotoxic activity

[CLC Number] R917 **[Document code]** A **[Article ID]** 2095-6975(2024)11-1020-10

Introduction

Bisabolane-type sesquiterpenoids, comprising a distinctive family of sesquiterpenoids, are present in both terrestrial plants and marine organisms. Characterized by a hexatomic ring with an aliphatic chain at the C-6 skeleton, these compounds, featuring various multi-functional groups and chiral centers, exhibit a wide range of bioactivities. These include antibacterial, anti-inflammatory, cytotoxic, antifouling, and vasorelaxant effects, which have garnered significant interest from chemists and pharmacologists [1]. Highly oxidized bisabolanes, particularly ester derivatives from acetic, angelic, and senecioic acid, represent a substantial and structurally diverse subset of this compound category, demonstrating fascinating biological activities [2-6].

The genus *Parasenecio* (Asteraceae) comprises approximately 60 species, primarily distributed in East Asia and the Himalayan region of China. Over 20 species of this genus have been utilized as traditional herbal medicines due to their antimicrobial, antitumor, and antioxidative properties [7-10]. Previous phytochemical studies on *Parasenecio* species have revealed the presence of numerous eremophilane-type sesquiterpenoids [11-17]. Our group investigated the chemical constituents from the ethyl acetate fraction of *Parasenecio rubescens* (S. Moore) Y. L. Chen, yielding 34 highly oxidized bisabolane-type sesquiterpenoids, with no eremophilane-type sesquiterpenoids detected [18-20]. Given that previous studies demonstrated the presence of eremophilane-type sesquiterpenoids as the main characteristic constituents of this genus, further investigation of the typical components of this species was considered particularly promising. To discover additional bisabolane-type sesquiterpenoids from *P. rubescens* and to identify bioactive and structurally novel natural products from this genus, a phytochemical study on the petroleum ether fraction of *P. rubescens* was conducted. This investigation resulted in the isolation of 14 previously undescribed highly oxidized bisabolane-type sesquiterpenoids (pararunines L–Y) and one known oplopane-type sesquiterpenoid. This paper presents the isolation, structure identification, and cytotoxic activities of these sesquiterpenoids.

[Received on] 23-Jan.-2024
[Research funding] This work was supported by the National Natural Science Foundation of China (Nos. 22077041, 81803847 and 31770380).
[*]**Corresponding author]** E-mail: ruanhl@mails.tjmu.edu.cn
[Δ]These authors contributed equally to this work.
These authors have no conflict of interest to declare.

Results and Discussion

Compound **1** (Fig. 1) was isolated as a colorless gum with a molecular formula of $C_{32}H_{46}O_{11}$, as deduced from the $[M + Na]^+$ ion peak at *m*/*z* 629.2943 (Calcd. for 629.2938) and ^{13}C nuclear magnetic resonance (NMR) data, indicating ten degrees of unsaturation.

The 1D NMR data (Tables 1 and 3) revealed characteristic signals for one acetoxy group [δ_H 2.01 (3H, s, H-2'''); δ_C 171.9 (C-1'''), 20.6 (C-2''')] and three angeloyloxy groups [δ_H 6.11 (1H, qq, J = 7.2, 1.3 Hz, H-3'), 1.98 (3H, dq, J = 7.2, 1.3 Hz, H-4') , 1.90 (3H, m, H-5'); δ_C 168.5 (C-1'), 128.8 (C-2'), 139.7 (C-3'), 16.1 (C-4'), 20.9 (C-5')], [δ_H 6.11 (1H, qq, J = 7.2, 1.3 Hz, H-3''), 1.98 (3H, dq, J = 7.2, 1.3 Hz, H-4'') , 1.85 (3H, m, H-5''); δ_C 167.8 (C-1''), 128.4 (C-2''), 140.3 (C-3''), 16.1 (C-4''), 20.7 (C-5'')], and [δ_H 6.17 (1H, qq, J = 7.2, 1.3 Hz, H-3''''), 1.95 (3H, dq, J = 7.2, 1.3 Hz, H-4'''') , 1.92 (3H, m, H-5''''); δ_C 168.3 (C-1''''), 129.1 (C-2''''), 139.7 (C-3''''), 16.2 (C-4''''), 21.0 (C-5'''')]. In addition to these four substituents, the ^{13}C NMR data, in conjunction with the heteronuclear single quantum coherence (HSQC) spectrum, indicated 15 additional skeletal carbon signals, comprising three methyls, two methylenes, seven methines (six oxygenated), and three quaternary carbons. Among these, resonances for a terminal double bond [δ_H 5.17, 5.37 (each 1H, s); δ_C 117.3 (CH_2) and 143.8 (C)] and an epoxy group [δ_H 3.17 (1H, br s); δ_C 64.2 (CH), 59.3 (C)] were readily discernible.

The planar structure of **1** (Fig. 1) was elucidated through

Table 1 ^1H NMR data of compounds 1–7 in CD_3OD (400 MHz, J in Hz)

Position	1	2	3	4	5	6	7
1	5.49 d (11.4)	5.40 d (11.2)	5.41 d (11.3)	5.47 d (11.1)	5.40 d (11.2)	5.40 d (11.2)	5.41 d (11.2)
2	3.17 s	3.15 s	3.15 s	3.14 s	3.17 s	3.15 s	3.15 s
4	5.54 d (4.6)	5.42 d (4.6)	5.42 d (4.6)	5.43 d (4.6)	5.41 d (4.5)	5.41 d (4.5)	5.46 d (4.8)
5	5.44 dd (4.6, 1.7)	5.16 dd (4.6, 1.7)	5.20 dd (4.6, 1.8)	5.35 dd (4.6, 1.7)	5.17 dd (4.5, 1.6)	5.16 (4.5, 1.7)	5.28 dd (4.8,1.8)
6	3.01 dd (11.4, 1.7)	2.97 dd (11.2, 1.7)	2.96 dd (11.3, 1.8)	2.98 dd (11.1, 1.7)	2.95 dd (11.2, 1.6)	2.96 dd (11.2, 1.7)	2.98 dd (11.2, 1.8)
8	5.67 t (7.1)	5.64 dd (11.7, 1.7)	5.63 dd (11.4, 1.6)	5.65 t (7.1)	5.63 dd (11.2, 1.4)	5.63 dd (11.4, 1.5)	5.65 overlap
9a	1.99 overlap	2.33 m	2.11 m	1.98 overlap	2.14 m	2.13 m	2.13 overlap
9b	1.80 m	1.50 overlap	1.42 m	1.78 m	1.41 m,	1.40 m	1.43 m
10	3.26 dd (9.7, 2.4)	3.52 dd (10.7, 1.5)	3.34 overlap	3.25 dd (9.8, 2.5)	3.43 overlap	3.43 dd (9.7, 1.3)	3.35 overlap
12	1.12 s	1.49 s	1.15 s	1.11 s	1.15s	1.14 s	1.13 s
13	1.14 s	1.54 s	1.12 s	1.13 s	1.09 s	1.09 s	1.10 s
14a	5.37 s	5.33 s	5.32 s	5.17 s	5.31 s	5.31 s	5.30 s
14b	5.17 s	5.14 s	5.12 s	5.38 s	5.12 s	5.12 s	5.10 s
15	1.34 s	1.33 s	1.33 s	1.33 s	1.33 s	1.33 s	1.33s
3'	6.11 qq (7.2, 1.3)	6.17 qq (7.2, 1.3)	6.16 qq (7.2, 1.3)	6.12 qq (7.2, 1.3)	6.16 qq (7.2, 1.3)	6.16 qq (7.2, 1.3)	6.15 qq (7.2, 1.3)
4'	1.98 dq (7.2, 1.3)	1.99 dq (7.2, 1.3)	1.99 dq (7.2, 1.3)	1.97 dq (7.2, 1.3)	1.99 dq (7.2, 1.3)	1.98 dq (7.2, 1.3)	1.98 dq (7.2, 1.3)
5'	1.90 m	1.91 m	1.92 m	1.90 m	1.91 m	1.91 m	1.92 m
2''		2.01 s	2.01 m	2.02 s	2.01 s	2.01 s	5.64 m
3''	6.11 qq (7.2, 1.3)						
4''	1.98 dq (7.2, 1.3)						2.21 q (7.4)
5''	1.85 m						1.09 t (7.4)
6''							2.16 d (1.2)
2'''	2.01 s	2.04 s	2.04 s	2.04 s	2.04 s	2.04 s	2.02 s
3''''	6.17 qq (7.2, 1.3)	6.17 qq (7.2, 1.3)	6.14 qq (7.2, 1.3)	6.11 qq (7.2, 1.3)	6.17 qq (7.2, 1.3)	6.16 qq (7.2, 1.3)	6.15 qq (7.2, 1.3)
4''''	1.95 dq (7.2, 1.3)	1.98 dq (7.2, 1.3)	1.98 dq (7.2, 1.3)	1.95 dq (7.2, 1.3)	1.98 dq (7.2, 1.3)	1.99 dq (7.2, 1.3)	1.98 dq (7.2, 1.3)
5''''	1.92 m	1.92 m	1.92 m	1.89 m	1.92 m	1.92 m	1.92 m
1'''''					3.44 overlap	3.20 s	
2'''''					1.13 t (7.0)		

Table 2 ^{1}H NMR data of compounds 8–14 in CD_3OD (400 MHz, J in Hz)

Position	8	9	10	11	12	13	14
1	5.41 d (11.2)	5.42 d (11.2)	5.42 d (11.2)	4.05 dd (11.6, 2.8)	5.45 dd (11.4, 2.8)	4.23 dd（11.2, 3.5）	4.12 dd (11.5, 3.4)
2	3.14 s	3.16 s	3.16 s	5.16 d (2.8)	3.74 d（2.8）	5.12 d（3.5）	5.21 d (3.4)
4	5.41 d (4.6)	5.53 d (4.5)	5.44 d (4.5)	3.64 d (2.8)	3.73 d（2.8）	5.17 d（3.5）	3.68 d (3.4)
5	5.19 dd (4.6, 1.6)	5.29 dd (4.5, 1.7)	5.27 dd (4.5, 1.7)	5.34 dd (11.6, 2.8)	5.42 dd (11.4, 2.8)	4.07 dd（11.2, 3.5）	5.37 dd (11.5, 3.4)
6	2.97 dd (11.2, 1.61)	3.01 dd (11.2, 1.7)	3.02 dd (11.2, 1.7)	3.03 t (11.6)	3.24 t (11.4)	2.77 t（11.2）	3.07 t (11.5)
8	5.57 dd (10.5, 3.2)	5.59 dd (10.4, 3.1)	5.51 dd (9.3, 4.3)	5.07 dd（8.3，4.1）	5.36 dd (8.3，4.2)	5.06 dd (9.1, 3.1)	5.29 dd (9.5, 3.3)
9a	1.63 m	2.05 m	2.04 overlap	2.55 m	2.49 m	2.65 m	2.08 overlap
9b	2.02 m	1.65 m	1.81 m	2.32 m	2.38 m	2.35 m	2.01 overlap
10	4.01 dd (9.8, 3.6)	4.02 dd (9.6, 3.4)	2.76 t (6.3)	5.14 overlap	5.09 m	5.22 overlap	3.59 dd (9.2, 1.5)
12	12a: 4.80 s; 12b: 4.90 s	12a: 4.80 s; 12b: 4.90 s	1.24 s	1.61 s	1.61 s	1.66 s	1.53 s
13	1.73 s	1.73 s	1.27 s	1.65 s	1.67 s	1.70 s	1.55 s
14a	5.30 s	5.29 s	5.35 s	5.16 s	5.30 s	5.28 s	5.25 s
14b	5.14 s	5.12 s	5.18 s	5.11 s	5.23 s	5.19 s	5.17 s
15	1.33 s	1.34 s	1.34 s	1.25 s	1.48 s	1.15 s	1.30 s
2'						2.08 s	
3'	6.15 qq (7.2, 1.3)	6.16 qq (7.2, 1.3)	6.17 qq (7.2, 1.3)	6.11 qq (7.2, 1.3)	6.07 qq (7.2, 1.3)		6.13 qq (7.2, 1.3)
4'	1.99 dq (7.2, 1.3)	1.99 dq (7.2, 1.3)	1.98 dq (7.2, 1.3)	2.01 dq (7.2, 1.3)	1.96 dq (7.2, 1.3)		2.01 dq (7.2, 1.3)
5'	1.91 m	1.94 m	1.93 m	1.87 m	1.89 m		1.95 m
2''	2.01 s		2.02 s	1.93 s	1.96 s		1.97 s
3''		6.15 qq (7.2, 1.3)				6.17 qq (7.2, 1.3)	
4''		1.96 dq (7.2, 1.3)				2.05 dq (7.2, 1.3)	
5''		1.85 m				2.01 m	
2'''	2.04 s	2.01 s	2.05 s				
3'''				6.11 qq (7.2, 1.3)	6.07 qq (7.2, 1.3)	6.17 qq (7.2, 1.3)	6.11 qq (7.2, 1.3)
4'''				1.95 dq (7.2, 1.3)	1.94 dq (7.2, 1.3)	1.97 dq (7.2, 1.3)	2.05 dq (7.2, 1.3)
5'''				1.87 m	1.87 m	1.90 m	1.97 m
3''''	6.15 qq (7.2, 1.3	6.16 qq (7.2, 1.3)	6.17 qq (7.2, 1.3)				
4''''	1.97 dq (7.2, 1.3)	1.98 dq (7.2, 1.3)	1.97 dq (7.2, 1.3)				
5''''	1.90 m	1.90 m	1.89 m				

Table 3 ^{13}C NMR data of compounds 1–14 in CD_3OD (100 MHz)

Position	1	2	3	4	5	6	7	8	9	10	11	12	13	14
1	68.6	69.3	69.2	68.7	69.3	69.3	69.2	69.3	69.3	69.3	73.0	76.0	69.4	73.2
2	64.2	63.9	63.9	64.1	63.9	64.0	64.1	64.0	64.1	63.9	77.1	76.4	77.6	76.9
3	59.3	59.1	59.0	59.1	59.1	59.1	59.3	59.1	59.3	59.1	73.9	72.6	73.0	73.8
4	72.5	72.8	72.7	72.8	72.8	72.8	71.8	72.8	72.4	72.8	74.7	76.3	76.6	74.8
5	69.3	69.5	69.5	69.4	69.5	69.5	69.6	69.5	69.5	69.4	74.8	75.4	71.8	75.0
6	43.3	42.5	42.7	43.2	42.6	42.5	42.9	42.4	42.6	42.7	41.9	38.1	46.9	41.4
7	143.8	145.1	145.4	143.8	145.4	145.4	145.5	144.9	144.9	144.6	148.8	147.4	148.7	149.6
8	77.2	75.7	75.6	77.2	75.8	75.8	75.6	75.7	75.6	75.8	79.1	76.7	78.9	77.1
9	36.0	37.7	37.1	36.0	37.0	36.9	37.2	40.8	40.8	34.4	32.8	33.1	33.3	37.7
10	76.3	75.6	75.2	76.4	73.8	73.5	75.3	72.7	72.7	62.4	121.1	120.7	121.6	76.0
11	73.6	73.6	73.2	73.6	77.9	78.1	73.4	149.0	149.0	60.2	136.0	135.1	134.9	73.9
12	24.9	27.8	25.5	24.9	22.3	21.7	25.0	111.3	111.3	24.9	18.2	18.1	18.1	28.2
13	26.0	30.0	25.0	26.0	21.0	20.2	25.6	17.8	17.8	19.0	26.0	26.0	26.0	29.9
14	117.3	116.7	116.3	117.5	116.3	116.4	116.1	116.8	116.7	117.1	111.5	113.8	112.5	111.5
15	19.0	18.9	18.9	18.9	18.9	18.9	18.9	18.9	19.1	18.8	24.0	24.4	23.5	24.0
1'	168.5	168.2	168.2	168.5	168.3	168.3	168.3	168.2	168.2	168.8	169.2	168.5	172.5	169.2
2'	128.8	128.5	128.5	128.8	128.5	128.5	128.9	128.4	128.4	128.6	129.5	129.6	23.5	129.6
3'	139.7	140.6	140.1	139.8	140.1	140.1	140.5	140.0	139.9	140.8	139.1	138.7		140.7
4'	16.1	16.2	16.2	16.1	16.3	16.2	16.3	16.2	16.0	16.2	16.1	16.1		16.3
5'	20.9	21.0	20.5	20.5	20.4	20.9	21.0	20.4	20.8	20.9	20.8	20.9		20.9
1''	167.8	172.0	171.5	171.6	171.6	172.0	166.8	171.6	167.8	171.6	172.1	172.0	168.7	172.1
2''	128.4	20.4	20.6	20.9	20.9	20.4	114.3	20.8	128.4	20.6	21.0	20.9	129.1	21.0
3''	140.3						164.9		140.2				139.5	
4''	16.1						34.7		16.2				16.2	
5''	20.7						12.3		20.6				21.3	
6''							19.0							
1'''	171.9	171.6	172.0	172.2	172.0	171.6	171.8	172.0	171.7	172.1	169.1	168.1	169.7	169.2
2'''	20.6	20.6	20.9	20.9	21.0	20.6	20.6	20.9	20.7	20.4	129.1	129.5	129.3	129.0
3'''											140.0	139.0	139.8	138.9
4'''											16.1	16.6	16.0	16.2
5'''											21.1	21.0	21.2	21.1
1''''	168.3	168.1	168.1	168.3	168.1	168.1	168.2	168.2	168.2	167.8				
2''''	129.1	128.7	128.8	129.1	128.8	128.8	140.0	128.8	128.9	128.4				
3''''	139.7	140.3	140.5	139.7	140.7	140.7	128.5	140.8	140.8	140.4				
4''''	16.2	16.3	16.2	16.1	16.2	16.1	16.1	16.2	16.2	16.1				
5''''	21.0	20.9	20.5	20.6	20.6	20.9	20.9	20.6	21.0	20.7				
1'''''					57.7	49.6								
2'''''					16.5									

analysis of its heteronuclear multiple bond correlation (HMBC) and ^{1}H-^{1}H correlation spectroscopy (COSY) data (Fig. 2). The ^{1}H-^{1}H COSY spectrum revealed two primary correlation fragments: CH(H-1)–CH(H-6)–CH(H-5)–CH(H-4) and CH(H-8)–CH_2(H-9)–CH(H-10). These fragments were connected to form a bisabolane sesquiterpenoid skeleton, as evidenced by HMBCs of H-1/C-7, C-3; H-2/C-6; H-5/C-7; H-6/C-14; H-8/C-14; H-10/C-12, C-13; H-15/C-4. The positions of three angeloyloxy groups and one acetoxy group were determined to be at C-1, C-4, C-8, and C-5, respectively, based on HMBCs from H-1, H-4, H-8, and H-5 to each of the corresponding carbonyls in the ester units (Fig. 2).

The relative configuration of the six-membered ring of **1** was elucidated through the nuclear overhauser effect spectroscopy (NOESY) correlations (Fig. 3), in conjunction with ^{1}H–^{1}H coupling constants. Assuming an α-orientation for H-6, H-1 was determined to be β-axial due to the large coupling constant ($J_{1,6}$ = 11.4 Hz) between H-1 and H-6, while H-5 was identified as α-equatorial based on the small coupling constant ($J_{5,6}$ = 1.7 Hz) between H-5 and H-6. Additionally,

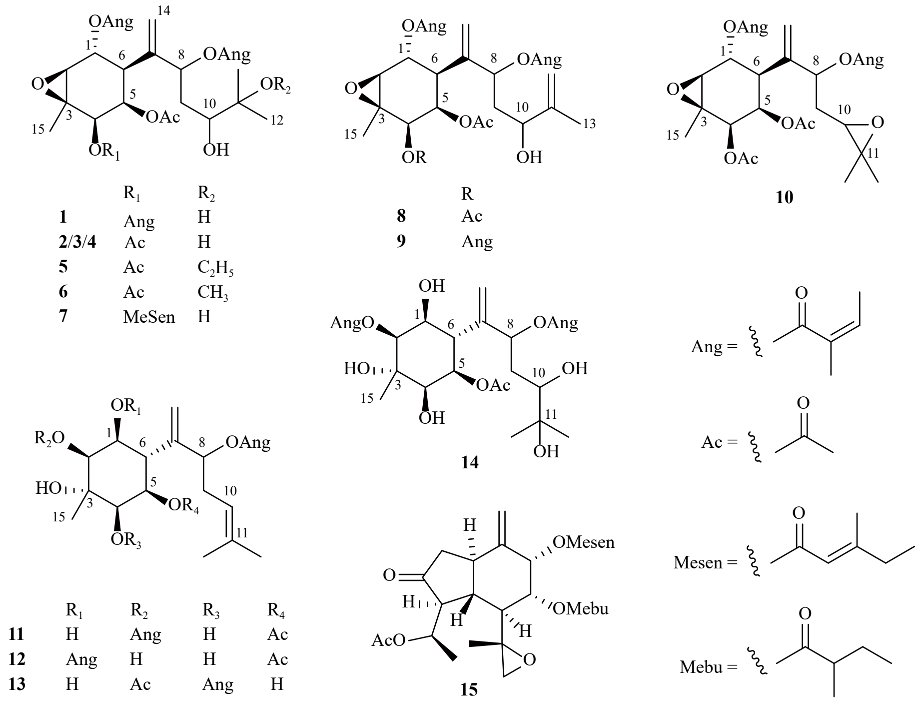

Fig. 1 Chemical structures of compounds 1–15.

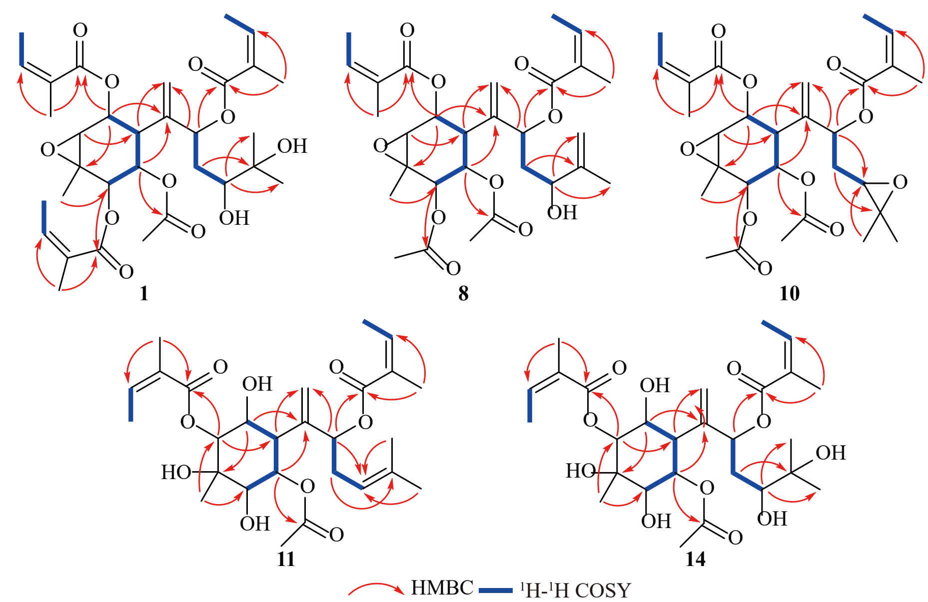

Fig. 2 ^{1}H-^{1}H COSY correlation and key HMBC of compounds 1, 8, 10, 11, and 14.

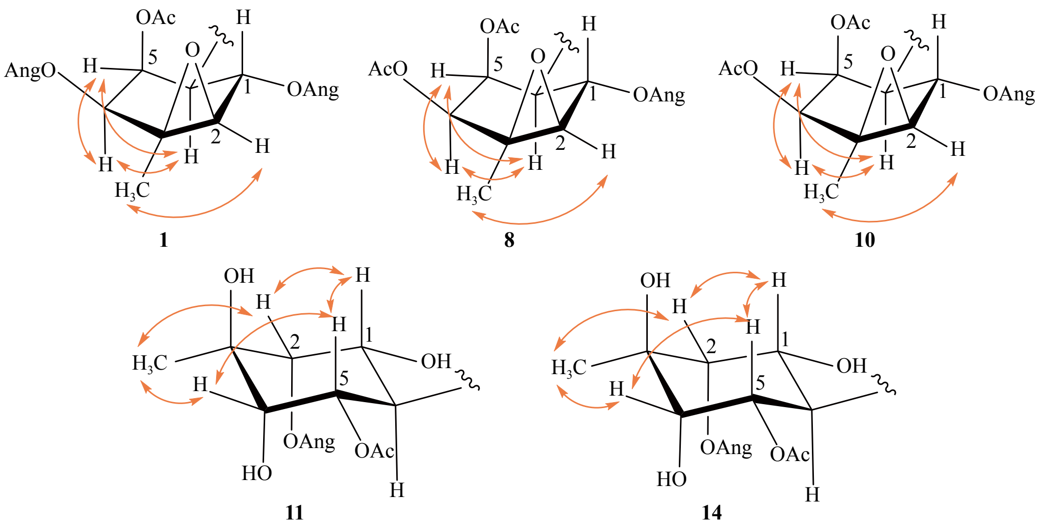

Fig. 3 Key NOESY correlations of compounds 1, 8, 10, 11, and 14.

the near-zero coupling constant between H-1 and H-2 indicated a dihedral angle of approximately 90°. This configuration suggests a twist-boat conformation for the cyclohexane ring, with the epoxy group at C-2 and C-3 in a β-orientation. The α-axial orientation of H-4 was confirmed by its NOESY correlation with H-6. However, the side chain's flexibility and the free rotation of the single bond between C-8 and C-10 precluded the determination of the optical configuration for the two stereogenic centers through NOESY experiments or electronic custom distributor (ECD) calculations. Consequently, the structure of **1** was established as depicted and named pararunine L.

Compound **2** yielded the molecular formula $C_{29}H_{42}O_{11}$, as determined by its high-resolution electrospray ionization mass spectrometry (HR-ESI-MS) peak at *m/z* 589.2628 $[M + Na]^+$ (Calcd. for $C_{29}H_{42}O_{11}Na$, 589.2625) and ^{13}C NMR data. The 1D NMR spectral data (Tables 1 and 3) of **2** exhibited similarities to those of **1**, with the primary distinction being the presence of an acetoxy group at C-4 in **2**, rather than an angeloyloxy group in **1**. This was confirmed through HMBC of H-4/C-1" (Fig. S18 in Supporting Information). **2** maintained the same relative configuration of the cyclohexane ring as **1** (twist-boat conformation), as evidenced by their NOESY correlations (Fig. S19 in Supporting Information) and ^1H NMR coupling constants (Table 1). Consequently, the structure of **2** was established as depicted in Fig. 1 and designated as pararunine M.

The molecular formulas of compounds **3** and **4** were both determined to be $C_{29}H_{42}O_{11}$ based on their HR-ESI-MS and ^{13}C NMR data. The 1D (Tables 1 and 3) and 2D (Fig. S26−S29 and S36−S39 in Supporting Information) NMR spectral data of **3** and **4** exhibited similarities to those of **2**. Analysis of their NOESY correlations and ^1H−^1H coupling constants data indicated that compounds **3** and **4** possessed the same relative configuration on the six-membered ring as **2**. Observed differences in the 1D NMR data and comparable optical rotation data suggested that compounds **2**, **3**, and **4** were diastereomers, differing in the configuration at the side chain. Consequently, the structures of **3** and **4** are elucidated in Fig. 1, and designated as pararunine N and pararunine O, respectively.

Compound **5** exhibited a molecular formula of $C_{31}H_{46}O_{11}$, as determined by HR-ESI-MS and ^{13}C NMR spectroscopic data. The NMR spectral data of **5** showed similarities to those of **2**, with the notable distinction of an ethoxy group at C-11 in **5** (Fig. S48 in Supporting Information). Consequently, the structure of **5** was definitively elucidated and designated as pararunine P.

Compound **6** exhibited a molecular formula of $C_{30}H_{44}O_{11}$, as determined by HR-ESI-MS, which aligned with its ^{13}C NMR spectral data. A comparative analysis of the NMR data between compounds **6** and **2** revealed structural similarities, with the notable distinction of an additional methoxy group at C-11 in **6**. This structural feature was corroborated by the HMBC of -OMe-11/C-11. By applying the same spectroscopic and computational methods used to determine the configuration of compound **1**, the relative configuration of **6** was similarly assigned. Consequently, the structure of **6** was established as illustrated and designated as pararunine Q.

Compound **7** yielded the molecular formula $C_{33}H_{48}O_{11}$, as determined by HR-ESI-MS and ^{13}C NMR data. The NMR spectral data (Tables 1 and 3) of **7** closely resembled those of **1**, with the notable difference that the angeloyloxy group at C-4 in **1** was substituted by a 4-methylsenecioyloxy group in **7**. An *E*-configured alkene was assigned based on a NOESY correlation between H-2" and H-4" (Fig. S69 in Supporting Information). The relative configuration of the six-membered ring was established using methods similar to those employed for **1**. Based on these findings, the structure of **7** was elucidated and designated as pararunine R.

The molecular formula of compound **8** was determined to be $C_{29}H_{40}O_{10}$, as confirmed by HR-ESI-MS and ^{13}C NMR data (Tables 2 and 3). Analysis of the NMR data for **8** indicated a structure similar to that of **2**. HMBCs from H-9 to C-11, H-10 to C-12, and H-13 to C-12 revealed that an additional double bond in the side chain was positioned between C-11 (δ_C 149.0) and C-12 (δ_C 111.3) (Fig. 2). The relative configuration of **8** was established through NOESY correlations and $^1H–^1H$ coupling constants, employing methods analogous to those used for compound **1**. Consequently, **8** was characterized as depicted and designated pararunine S.

Compound **9** displayed an angeloyloxy group [δ_H 6.15 (1H, qq, J = 7.2, 1.3 Hz, H-3''), 1.96 (3H, dq, J = 7.2, 1.3 Hz, H-4'') , 1.85 (3H, m, H-5''); δ_C 167.8 (C-1''), 128.4 (C-2''), 140.2 (C-3''), 16.2 (C-4''), 20.6 (C-5'')] at C-4, substituting the acetoxy group in **8**. This substitution was further corroborated by the HR-ESI-MS ion peak at *m/z* 611.2834 $[M + Na]^+$ (Calcd. for $C_{32}H_{44}O_{10}Na$, 611.2832) and HMBC analysis. Through comparison of the coupling constants and comprehensive analysis of the 2D NMR data to **8**, the structure of **9** was elucidated as depicted and designated pararunine T.

Compound **10** yielded an ion peak at *m/z* 566.2952 $[M + NH_4]^+$, consistent with a molecular formula of $C_{29}H_{44}NO_{10}$, indicating ten degrees of unsaturation. A comparison of its 1D and 2D NMR spectral data with those of **2** revealed a similar planar structure, with the exception of an additional epoxy group at C-10 and C-11 in **10**. This structural feature was corroborated by the HMBCs of H-8, H-12/C-10 and H-9/C-11 (Fig. 2). Consequently, the structure of **10** was elucidated and designated as pararunine U.

Compound **11** exhibited the molecular formula $C_{27}H_{40}O_9$ with eight indices of hydrogen deficiency, as determined from the HR-ESI-MS and ^{13}C NMR data. A comparison of the NMR data of **11** with those of **1** revealed a similar bisabolane-type sesquiterpenoid skeleton, with the notable absence of an epoxy group in **11**. Additionally, Compound **11** contained an additional olefinic resonance, identified as a Δ^{10} moiety through HMBCs of H-8, H-12, H-13/C-10 and H-9/C-11 (Fig. 2). Moreover, HMBCs from H-2 to C-1', from H-8 to C-1''', and from H-5 to C-1'' indicated that the two angeloyloxy groups and one acetoxy group of **11** were attached at C-2, C-8, and C-5, respectively.

The stereochemistry of **11** was proposed to be identical to that of pararubin A [19], for which the relative configuration was established through comparison of the coupling constants, NOESY correlations, and biogenetic considerations. To provide conclusive evidence, H-6 was arbitrarily designated as having an α-orientation. Consequently, H-1 and H-5 were determined to possess β-orientations based on the large $J_{1,6}$ (11.4 Hz) and $J_{5,6}$ (11.4 Hz) values. Furthermore, H-2 and H-4 were deduced to be β-equatorial due to the small coupling constants of $J_{1,2}$ (2.8 Hz) and $J_{4,5}$ (2.8 Hz) (Fig. 3). Thus, the structure of **11** was elucidated and designated as pararunine V.

Compounds **12** and **13** were determined to share the same molecular formula as **11** based on their respective ^{13}C NMR and HR-ESI-MS data. The NMR spectra of **12** and **13** exhibited notable similarities to those of **11**, suggesting that **12** and **13** possessed an identical bisabolane skeleton with two angeloyloxy groups and one acetoxy group. The positions of these groups were elucidated through HMBCs: H-1/C-1', H-8/C-1''', and H-5/C-1'' for **12**; and H-4/C-1'', H-8/C-1''', and H-2/C-1' for **13**. The relative configurations of **12** and **13** were confirmed to be consistent with that of **11**, as evidenced by their identical coupling constants and NOESY data. Consequently, the structures of compounds **12** (pararunine W) and **13** (pararunine X) were established as depicted.

The molecular formula of compound **14** was determined to be $C_{27}H_{42}O_{11}$ based on HR-ESI-MS and ^{13}C NMR data. The characteristic 1D and 2D NMR spectral analysis revealed that **14** possessed a structure similar to that of **11**, with the notable distinction of two additional hydroxy groups at C-**10** and C-**11**, respectively. Consequently, the structure of **14** (pararunine Y) was elucidated as depicted.

The known compound songaricalarin E (**15**) was isolated and identified through comparison of its physical and spectroscopic characteristics with the data published in the literature [21].

Compounds **1−14** are classified as highly oxygenated bisabolane-type sesquiterpenoids, some of which have been previously reported to exhibit varying degrees of cytotoxic activities [1, 6]. Consequently, all isolated sesquiterpenoids were evaluated for *in vitro* cytotoxicity against four human cancer cell lines (MCF-7, HeLa, HCT116, and HT-29) using the MTT assay, with doxorubicin as a positive control (Table S1 in Supporting Information). The subsequent cytotoxicity assay (Table 4) revealed that pararunine Q (6) exhibited weak cytotoxicities against the HeLa and HCT116 cell lines. Pararunine U (**10**) demonstrated minimal cytotoxicity against the HT-29 cell line, while pararunine V (**11**) showed weak activity against the MCF-7, HeLa, and HCT116 cell lines. Notably, songaricalarin E (**15**) displayed cytotoxic effects against the MCF-7, HCT116, and HT-29 cell lines. It is noteworthy that **15** was previously reported to be active against human breast adenocarcinoma (MCF-7), epidermoid carcinoma of the nasopharynx (KB), human lung carcinoma (A-549), and vincristine-resistant nasopharyngeal (KBVIN) cell lines.

Experimental

General experimental procedures

CD and UV data were obtained using a JASCO-810 spectrometer in MeOH. IR spectra were acquired with a Thermo Scientific Nicolet iS50R FT-IR spectrophotometer. Optical rotations were measured on a PerkinElmer 341 polarimeter in MeOH. HR-ESI-MS data were collected using a Thermo Scientific LTQ-Orbitrap XL mass spectrometer. NMR spectra were recorded on a Bruker-AM-400 spectrometer, with tetramethylsilane (TMS) as the internal standard. Column chromatography utilized silica gel (200–300 or 300–400 mesh; Qingdao Marine Chemical Inc.), MCI gel (CHP20P, 75–150 μm; Mitsubishi Chemical Industries Ltd.), and Sephadex LH-20 gel (GE Healthcare). Medium-pressure

Table 4 Cytotoxic activities of compounds 1–15

Compounds	IC_{50} ($\mu mol\cdot L^{-1}$) ± SD			
	MCF-7	HeLa	HCT116	HT-29
1	> 50	> 50	> 50	> 50
2	> 50	> 50	> 50	> 50
3	> 50	> 50	> 50	> 50
4	> 50	> 50	> 50	> 50
5	> 50	> 50	> 50	> 50
6	> 50	36.66 ± 0.86	34.4 ± 0.87	> 50
7	> 50	> 50	> 50	> 50
8	> 50	> 50	> 50	> 50
9	> 50	> 50	> 50	> 50
10	> 50	> 50	> 50	49.00 ± 1.32
11	41.40 ± 0.54	45.31 ± 1.48	48.7 ± 0.73	> 50
12	> 50	> 50	> 50	> 50
13	> 50	> 50	> 50	> 50
14	> 50	> 50	> 50	> 50
15	34.64 ± 0.72	> 50	46.1 ± 1.14	49.60 ± 1.71
Doxorubicin [b]	0.44 ± 0.49	0.31 ± 0.92	2.47 ± 0.82	2.53 ± 0.53

[a] Results are the means of three independent assays. [b] Positive control.

liquid chromatography (MPLC) was performed on a Sepa-Bean machine U chromatography system using the Sepa-Flash Spherical C_{18} column (420 g, 20−45 μm; Santai Science Inc.). HPLC separations were conducted on an Agilent 1220 system with a UV detector and semipreparative columns (5 μm, 10 mm × 250 mm, YMC-Pack ODS-A or SIL-06) at a flow rate of 2.0 $mL\cdot min^{-1}$. MTT assays were performed on a Bio-Tek Synergy 2 multimode microplate reader (Gene Company Ltd.).

Plant material

The entire plant of *P. rubescens* was collected from Mount Lushan in Jiujiang City, Jiangxi Province, China, in September 2012. Research scientist HUANG Beili (Lushan Botanical Garden) identified the specimen. A voucher specimen (No. 20120901) has been deposited in the Herbarium of Materia Medica at the School of Pharmacy, Tongji Medical College of Huazhong University of Science and Technology.

Extraction and isolation

The air-dried plant materials of *P. rubescens* (18.4 kg) were pulverized and extracted five times with 90% acetone (5 × 50 L, three days each time) at room temperature to obtain the crude extract. This extract was then suspended in water and successively partitioned with petroleum ether, ethyl acetate, and *n*-butyl alcohol. The petroleum ether extract (280.0 g) was separated by a silica gel column (10 cm × 120 cm, 200–300 mesh, 2.5 kg) eluting with a gradient of petroleum ether/ EtOAc (20 : 1 to 0 : 100) to obtain 12 major fractions (Fr. PA-PL). Fr. PC (29.2 g), Fr. PF (31.2 g), and Fr. PG (27.3 g) were applied to the MCI gel column eluted with MeOH/H_2O (50 : 50 to 100 : 0) to yield 6 (Fr. PC1 to PC6), 8 (Fr. PF1 to PF8), and 6 (Fr. PG1 to PG6) subfractions respectively. Fr. PC3 (8.1 g) was separated on an ODS C_{18} column (420 g, 20−45 μm) by MPLC eluted with gradient MeOH/H_2O (50 : 50 to 100 : 0) to yield 12 subfractions (Fr. PC3-1 to PC3-12). Fr. PC3-4 (1.3 g) was subjected to semipreparative reverse phase HPLC (MeOH/H_2O, 60 : 40) and then further purified by semipreparative normal phase HPLC (*n*-hexane/isopropanol, 90 : 10) to yield **2** (15.4 mg, t_R 26.7 min), **3** (12.1 mg, t_R 32.0 min), and **9** (3.1 mg, t_R 39.4 min). Fr. PC3-6 (1.4 g) was purified using the same method as Fr. PC3-4 to afford **4** (7.8 mg, t_R 19.2 min), **5** (5.4 mg, t_R 21.1 min), and **8** (6.4 mg, t_R 26.1 min). Fr. PF4 (7.6 g) was fractionated using a Sephadex LH-20 column (CH_2Cl_2/MeOH, 1 : 1) to obtain six subfractions, Fr. PF4-1 to PF4-6. Fr. PF4-2 (1.6 g) was subsequently applied to semipreparative reverse phase HPLC (MeOH/H_2O, 60 : 40) to afford **1** (8.1 mg, t_R 25.2 min) and **7** (3.5 mg, t_R 37.8 min). Fr. PF4-5 (0.7 g) was applied to semipreparative normal phase HPLC (*n*-hexane/isopropanol, 90 : 10) to yield **11** (5.8 mg, t_R 35.3 min), while Fr. PF4-6 (0.9 g) was also subjected to semipreparative normal phase HPLC (*n*-hexane/isopropanol, 90 : 10) to give **10** (6.4 mg, t_R 28.3 min) and **12** (7.5 mg, t_R 31.2 min). Fr. PG-4 (8.5 g) was isolated by ODS MPLC (420 g, 20−45 μm) to obtain 15 subfractions (Fr. PG-4-1 to PG-4-15). **15** (12.3 mg) was crystallized in methanol from Fr. PG-4-3. Fr. PG-4-5 (0.9 g) was separated by normal phase HPLC (*n*-hexane/isopropanol, 95 : 15) to obtain **6** (6.3 mg, t_R 25.2 min) and **13** (6.9 mg, t_R 45.9 min). Fr. PG-4-5 (1.3 g) was repeatedly purified by semipreparative reverse phase HPLC (70% and 50% MeOH−H_2O, successively) to afford **14** (11.7 mg, t_R 45.1 min).

Spectroscopic data of compounds

Pararunine L (**1**): Colorless gums; $[\alpha]_D^{20}$ −28 (*c* 0.11, CH_3OH); UV (MeOH) λ_{max} (log ε) 213 (4.38) nm; IR (KBr) ν_{max} 3509, 2976, 2931, 1749, 1721, 1647, 1458, 1439, 1383 cm^{-1}; ^1H and ^{13}C NMR data (Tables 1 and 2); (+)-HR-ESI-MS *m/z* 629.2943 $[M + Na]^+$ (Calcd. for $C_{32}H_{46}O_{11}Na$, 629.2938).

Pararunine M (**2**): Colorless gums; $[\alpha]_D^{20}$ −37 (*c* 0.31, CH_3OH); UV (CH_3OH) λ_{max} (log ε) 216 (4.33) nm; IR (KBr) ν_{max} 3466, 2980, 2935, 1749, 1716, 1649, 1458, 1437, 1377 cm^{-1}; ^1H and ^{13}C NMR data (Tables 1 and 2); HR-ESI-MS *m/z* 589.2628 $[M + Na]^+$ (Calcd. for $C_{29}H_{42}O_{11}Na$, 589.2625).

Pararunine N (**3**): Colorless gums; $[\alpha]_D^{20}$ −23 (*c* 0.09, CH_3OH); UV (CH_3OH) λ_{max} (log ε) 217 (4.34) nm; IR (KBr) ν_{max} 3512, 2977, 2932, 1750, 1721, 1647, 1458, 1437, 1371 cm^{-1}; ^1H and ^{13}C NMR data (Tables 1 and 2); HR-ESI-MS *m/z* 589.2628 $[M + Na]^+$ (Calcd. for $C_{29}H_{42}O_{11}Na$, 589.2625).

Pararunine O (**4**): Colorless gums; $[\alpha]_D^{20}$ −51 (*c* 0.29, CH_3OH); UV (CH_3OH) λ_{max} (log ε) 218 (4.37) nm; IR (KBr) ν_{max} 3516, 2976, 2928, 1750, 1721, 1648, 1457, 1438, 1383, 1370 cm^{-1}; ^1H and ^{13}C NMR data (Tables 1 and 2); HR-ESI-MS *m/z* 589.2628 $[M + Na]^+$ (Calcd. for $C_{29}H_{42}O_{11}Na$, 589.2625).

Pararunine P (**5**): Colorless gums; $[\alpha]_D^{20}$ −26 (*c* 0.06, CH_3OH); UV (MeOH) λ_{max} (log ε) 219 (4.28) nm; IR (KBr) ν_{max} 3486, 2974, 2932, 1750, 1721, 1648, 1458, 1439, 1384, 1359 cm^{-1}; ^1H and ^{13}C NMR data (Tables 1 and 2); HR-ESI-MS *m/z* 612.3372 $[M + NH_4]^+$ (Calcd. for $C_{31}H_{50}NO_{11}$, 612.3384).

Pararunine Q (**6**): Colorless gums; $[\alpha]_D^{20}$ −23 (*c* 0.12, CH_3OH); UV (CH_3OH) λ_{max} (log ε) 214 (4.28) nm; IR (KBr) ν_{max} 3477, 2973, 2928, 1722, 1705, 1647, 1457, 1382, 1359 cm^{-1}; ^1H and ^{13}C NMR data (Tables 1 and 3); HR-ESI-MS *m/z* 598.3217 $[M + NH_4]^+$ (Calcd. for $C_{30}H_{48}NO_{11}$, 598.3227).

Pararunine R (**7**): Colorless gums; $[\alpha]_D^{20}$−29 (*c* 0.11, CH_3OH); UV (CH_3OH) λ_{max} (log ε) 217 (4.39) nm; IR (KBr) ν_{max} 3546, 2977, 2930. 1749, 1720, 1648, 1459, 1373, cm^{-1}; ^1H and ^{13}C NMR data (Tables 1 and 3); HR-ESI-MS *m/z* 643.3100 $[M + Na]^+$ (Calcd. for $C_{33}H_{48}O_{11}Na$, 643.3094).

Pararunine S (**8**): Colorless gums; $[\alpha]_D^{20}$ −36 (*c* 0.05, CH_3OH); UV (CH_3OH) λ_{max} (log ε) 216 (4.49) nm; IR (KBr) ν_{max} 3486, 2976, 2931, 1749, 1720, 1647, 1458, 1437, 1383, 1371 cm^{-1}; ^1H and ^{13}C NMR data (Tables 2 and 3); HR-ESI-MS *m/z* 571.2530 $[M + Na]^+$ (Calcd. for $C_{29}H_{40}O_{10}Na$, 571.2519).

Pararunine T (**9**): Colorless gums; $[\alpha]_D^{20}$ −24 (*c* 0.12, CH_3OH); UV (CH_3OH) λ_{max} (log ε) 218 (4.42) nm; IR (KBr) ν_{max} 3482, 2958, 2927, 1750, 1722, 1648, 1457, 1384, 1359 cm^{-1}; ^1H and ^{13}C NMR data (Tables 2 and 3); HR-ESI-MS *m/z* 611.2834 $[M + Na]^+$ (Calcd. for $C_{32}H_{44}O_{10}Na$, 611.2832).

Pararunine U (**10**): Colorless gums; $[\alpha]_D^{20}$ −20 (*c* 0.03, CH_3OH); UV (CH_3OH) λ_{max} (log ε) 216 (4.28) nm; IR (KBr) ν_{max} 3478, 2977, 2931, 1750, 1721, 1647, 1457, 1437, 1383, 1369 cm^{-1}; ^1H and ^{13}C NMR data (Tables 2 and 3); HR-ESI-MS *m/z* 566.2952 $[M + NH_4]^+$ (Calcd. for $C_{29}H_{44}NO_{10}$, 566.2965).

Pararunine V (**11**): Colorless gums; $[\alpha]_D^{20}$ −31 (*c* 0.07, CH_3OH); UV (CH_3OH) λ_{max} (log ε) 212 (4.34) nm; IR (KBr) ν_{max} 3466, 2974, 2928, 1717, 1648, 1457, 1440, 1382, 1359 cm^{-1};^1H and ^{13}C NMR data (Tables 2 and 3); HR-ESI-MS *m/z* 531.2576 $[M + Na]^+$ (Calcd. for $C_{27}H_{40}O_9Na$, 531.2570).

Pararunine W (**12**): Colorless gums; $[\alpha]_D^{20}$ −28 (*c* 0.16, CH_3OH); UV (CH_3OH) λ_{max} (log ε) 213 (4.32) nm; IR (KBr) ν_{max} 3447, 2973, 2928, 1718, 1648, 1457, 1439, 1383, 1358 cm^{-1}; ^1H and ^{13}C NMR data (Tables 2 and 3); HR-ESI-MS *m/z* 531.2578 $[M + Na]^+$ (Calcd. for $C_{27}H_{40}O_9Na$, 531.2570)

Pararunine X (**13**): Colorless gums; $[\alpha]_D^{20}$ −21 (*c* 0.08, CH_3OH); UV (CH_3OH) λ_{max} (log ε) 216 (4.35) nm; IR (KBr) ν_{max} 3481, 2976, 2933, 1750, 1721, 1647, 1458, 1437, 1370 cm^{-1}; ^1H and ^{13}C NMR data (Tables 2 and 3); HR-ESI-MS *m/z* 531.2568 $[M + Na]^+$ (Calcd. for $C_{27}H_{40}O_9Na$, 531.2570)

Pararunine Y (**14**): Colorless gums; $[\alpha]_D^{20}$ −40 (*c* 0.14, CH_3OH); UV (CH_3OH) λ_{max} (log ε) 214 (4.36) nm; IR (KBr) ν_{max} 3443, 2977, 2932, 1701, 1648, 1458, 1439, 1383, 1356 cm^{-1}; ^1H and ^{13}C NMR data (Tables 2 and 3); HR-ESI-MS *m/z* 565.2627 $[M + Na]^+$ (Calcd. for $C_{27}H_{42}O_{11}Na$, 565.2625)

Cytotoxicity assays

Cytotoxicity assays were conducted using a panel of four human cancer cell lines, including MCF-7 (breast cancer), HeLa (cervical cancer), HT-29 (colon cancer cell line), and HCT116 (colorectal carcinoma). Cell viability was assessed using the MTT method (S3 in Supporting Information) as previously described [22]. The IC_{50} values were calculated from the MTT viability curves using GraphPad Prism software. Doxorubicin hydrochloride served as the positive control. The reported results were derived from three independent experiments.

Conclusions

In conclusion, this study isolated 14 previously uncharacterized highly oxidized bisabolane-type sesquiterpenoids, named pararunine L–Y, along with one known oplopane-type sesquiterpenoid from the whole plant of *P. rubescens*. While eremophilane-type sesquiterpenoids are typically considered characteristic constituents of the genus, this research demonstrates that *P. rubescens* contains a significant abundance of bisabolane-type sesquiterpenoids. These findings significantly enhance the chemical diversity known within this genus, underscoring the importance of further exploration into the potential pharmacological properties of bisabolane-type sesquiterpenoids.

References

[1] Shu HZ, Peng C, Bu L, *et al*. Bisabolane-type sesquiterpenoids:

structural diversity and biological activity [J]. *Phytochemistry*, 2021, **192**: 112927.
[2] Zhu Y, Yang L, Jia ZJ. Novel highly oxygenated bisabolane sesquiterpenes from *Cremanthodium discoideum* [J]. *J Nat Prod*, 1999, **62**(11): 1479-1483.
[3] Su BN, Zhu QX, Jia ZJ. Nor-lignan and sesquiterpenes from *Cremanthodium ellisii* [J]. *Phytochemistry*, 2000, **53**(8): 1103-1108.
[4] Liu CM, Fei DQ, Wu QH, *et al*. Bisabolane sesquiterpenes from the Roots of *Ligularia cymbulifera* [J]. *J Nat Prod*, 2006, **69**(4): 695-699.
[5] Liu CM, Wang HX, Wei SL, *et al*. Pyrrolizidine alkaloids and bisabolane sesquiterpenes from the Roots of *Ligularia cymbulifera* [J]. *Helvetica Chimica Acta*, 2008, **91**(2): 308-316.
[6] Wang Q, Chen TH, Bastow KF, *et al*. Altaicalarins A− D, cytotoxic bisabolane sesquiterpenes from *Ligularia altaica* [J]. *J Nat Prod*, 2010, **73**(2): 139-142.
[7] Zhang ML, Zhang JJ, Huo CH, *et al*. Chemical constituents of plants from the genus *Cacalia* [J]. *Chem Biodivers*, 2010, **7**(1): 105-115.
[8] Hou C, Kulka M, Zhang J, *et al*. Occurrence and biological activities of eremophilane-type sesquiterpenes [J]. *Mini-Rev Med Chem*, 2014, **14**(8): 664-677.
[9] Kwon Y, Cho SY, Kwon J, *et al*. Anti-atopic dermatitis effects of *Parasenecio auriculatus via* simultaneous inhibition of multiple inflammatory pathways [J]. *BMB Rep*, 2022, **55**(6): 275.
[10] Cho EJ, Choi JY, Lee KH, *et al*. Isolation of antibacterial compounds from *Parasenecio pseudotaimingasa* [J]. *Hortic Environ Biote*, 2012, **53**(6): 561-564.
[11] Zhou M, Duan FF, Gao Y, *et al*. Eremophilane sesquiterpenoids from the whole plant of *Parasenecio albus* with immunosuppressive activity [J]. *Bioorg Chem*, 2021, **115**: 105247.
[12] Liu T, Wu H, Zhang J, *et al*. Modified eremophilanes from *Parasenecio hastatus* and their neuroprotective activities [J]. *J Nat Prod*, 2020, **83**(2): 185-193.
[13] Zhou M, Zhou J, Liu J, *et al*. Parasubindoles A−G, seven eremophilanyl indoles from the whole plant of *Parasenecio albus* [J]. *J Org Chem*, 2018, **83**(19): 12122-12128.
[14] Pang XY, Li YX, Gong Y, *et al*. Sesquiterpenes from the whole plants of *Parasenecio roborowskii* [J]. *Fitoterapia*, 2017, **116**: 24-33.
[15] Huang GD, Yang YJ, Wu WS, *et al*. Terpenoids from the aerial parts of *Parasenecio deltophylla* [J]. *J Nat Prod*, 2010, **73**(11): 1954-1957.
[16] Mao MJ, Yang ZD, Jia ZJ. New eremophilane sesquiterpenes from *Cacalia ainsliaeflora* [J]. *Planta Med*, 2003, **69**(8): 745-749.
[17] Mao MJ, Jia ZJ. Eremophilane sesquiterpenes from *Cacalia ainsliaeflora* [J]. *Planta Med*, 2002, **68**(1): 55-59.
[18] Jin A, Duan FF, Chang JL, *et al*. Chlorinated bisabolene sesquiterpenoids from the whole plant of *Parasenecio rubescens* [J]. *Fitoterapia*, 2022, **156**: 105093.
[19] Jin A, Wu WM, Yu HY, *et al*. Bisabolane-type sesquiterpenoids from the whole plant of *Parasenecio rubescens* [J]. *J Nat Prod*, 2015, **78**(8): 2057-2066.
[20] Jin A, Wu WM, Ruan HL. Sesquiterpenoids and monoterpenoid coumarins from *Parasenecio rubescens* [J]. *RSC Adv*, 2017, **7**: 5167-5176.
[21] Wang Q, Chen TH, Bastow KF, *et al*. Songaricalarins A-E, cytotoxic oplopane sesquiterpenes from *Ligularia songarica* [J]. *J Nat Prod*, 2013, **76**(3): 305-310.
[22] Duan FF, Gao Y, Peng XG, *et al*. [11]-chaetoglobosins with cytotoxic activities from *Pseudeurotium bakeri* [J]. *Bioorg Chem*, 2022, **127**: 106011.

Cite this article as: JIN An, DUAN Fangfang, RUAN Hanli. Highly oxidized sesquiterpenoids from *Parasenecio rubescens* and assessment of their cytotoxicity [J]. *Chin J Nat Med*, 2024, **22**(11): 1020-1029.